

Recent developments on cavity ring-down spectroscopy with tunable cw lasers in the mid-infrared

M. Mürtz^{*a}, T. Kayser^b, D. Kleine^a, S. Stry^a, P. Hering^a, W. Urban^b

^aInstitut für Lasermedizin, Universität Düsseldorf, 40225 Düsseldorf

^bInstitut für Angewandte Physik, Universität Bonn, 53115 Bonn

ABSTRACT

We report on our recent advances with cavity ring-down spectroscopy using mid-infrared cw lasers. An external high-finesse cavity is excited on a single fundamental mode with a tunable laser operating in the $3\mu\text{m}$ region. After excitation the laser power is turned off for a short time and the subsequent decay of the field stored inside the cavity is observed. The effective pathlength covered by the laser light inside the cavity during the decay amounts to several km, depending on the mirror reflectivity. Measurement of the decay time gives the photon losses and thus enables the detection of weakly absorbing species inside the cavity. This approach is closely related to cavity ring-down spectroscopy with pulsed lasers. However the cw approach exhibits several advantages concerning spectral resolution and detection sensitivity. Application of this method to online monitoring of trace gases seems to be very promising. We demonstrate detection of hydrocarbons, like methane and ethylene on the ppb level.

Keywords: cavity ring-down, infrared spectroscopy, CO laser, trace gas detection, hydrocarbons

1. INTRODUCTION

The problem of detecting weakly absorbing species can be addressed by a variety of methods. Cavity ring-down spectroscopy (CRDS) is one of the most sensitive methods to obtain absorption spectra of diluted gas samples.¹⁻⁵ A ring-down cavity (RDC) consists of a pair of high-reflectivity mirrors forming an optical cavity. A laser pulse is sent to the RDC and the down-ringing of this pulse is observed with a photodetector. The decay rate is characteristic for the photon losses experienced by the pulse traveling forth and back between the RDC mirrors. A RDC can thus be considered as a multi-pass cell with a huge optical pathlength. Effective pathlengths of more than 100 km have been achieved with a 1m-long cell.⁵ This technique is now widely employed for high-sensitivity applications from the UV to the near-infrared.⁶⁻¹¹ In the mid-infrared, CRDS has found less applications due to the lack of very-high reflectivity mirrors and poor photodetector performance.^{12,13} However, the situation can be considerably improved if a sufficiently narrow-linewidth cw laser is used to excite the RDC.¹⁴⁻²⁰ With this cw approach almost 100% of the laser light is transmitted to the photodetector, whereas with pulsed CRDS most of the incident laser light is wasted by reflection at the input mirror. Thus, the cw approach is ideally suited to be combined with low-power tunable MIR laser sources. Furthermore, this technique is not affected by laser amplitude noise and also provides much better spectral resolution than the traditional pulsed CRDS. In order to study the benefits of the cw CRDS approach in the mid-infrared region we started an experimental study utilizing a narrow-linewidth CO₂ laser in 1997. We demonstrated the feasibility of the method and showed that absorption coefficients as low as $10^{-8}/\text{cm}$ are detectable.²¹ In the present work we studied the performance of a cw-CRDS setup in the spectral region around $3\mu\text{m}$. This wavelength region is of great interest since it is the fingerprint region of many important molecules of atmospheric relevance. Currently, several novel tunable laser sources for this spectral region are being developed, such as III-V semiconductor lasers and nonlinear conversion devices. In this work we employed a tunable CO sideband laser to continuously excite a RDC. We describe the experimental arrangement and results, and discuss the benefits and difficulties of this approach.

*Correspondence: E-mail: m.muertz@iap.uni-bonn.de

2. HIGH-RESOLUTION RING-DOWN SPECTROSCOPY WITH CW LASERS

The basic experimental arrangement for CRDS with a cw laser is shown in Fig. 2.1. A tunable laser is directed via a fast optical switch towards a high-finesse optical cavity. Commonly, the cavity mirrors are arranged in a stable near-confocal geometry. This gives a regular mode pattern (Fig. 2.2) with a free spectral range (FSR) of 150 MHz for a 1m-long RDC. If the laser frequency is tuned to one of the cavity resonance modes, intensity builds up inside the cavity due to the coherent cw excitation. After reaching steady state, the laser power is turned off by means of the fast optical switch and the leak-out of the energy stored inside the cavity is detected by the photodetector behind the RDC. The decay of the radiation is usually recorded with a digital storage oscilloscope. With single mode excitation the energy decay is single exponential and the decay rate $1/\tau$ is given by:

$$1/\tau = c(1-R)/d + \alpha,$$

where c is the speed of light, d is the length of the RDC, R is the reflectivity of the mirrors, and α is the absorption coefficient of the medium between the mirrors. The first term describes the mirror losses, the second term describes the losses introduced from an absorber sample inside the cavity.

Ideally, 100% of the incident radiation is transmitted to the detector due to the coherent build-up on resonance. Thus, a very high signal-to-noise ratio of the intensity decay recording is achievable. This is of great importance in the mid-infrared region because the signal detection suffers from thermal-background limited detector performance. In reality, the photon losses due to absorption and scattering in the mirrors reduce the fraction of light transmitted. Also, there are difficulties with coherently exciting a single mode of the high-finesse cavity due to the frequency jitter of laser and cavity. If the laser linewidth during the build-up phase is larger than the resonance width of the cavity mode only a small fraction

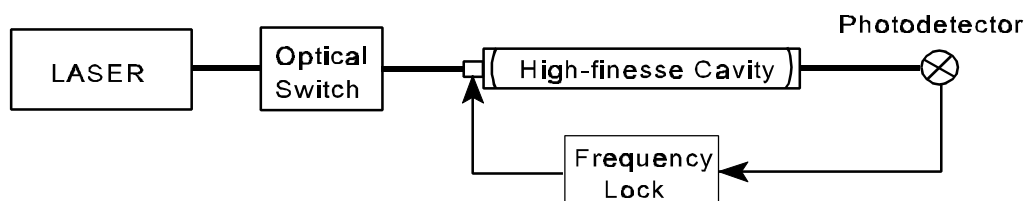


Fig. 2.1: Basic arrangement for cavity ring-down spectroscopy with a cw laser.

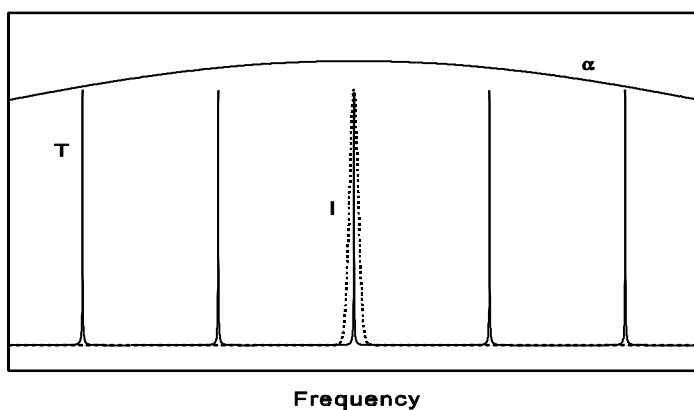


Fig. 2.2: Illustration of the spectral situation and linewidth relations in this work, α : line profile of absorbing medium, T: transmission of cavity, l: line profile of laser emission (dotted line).

of the incident light will be coupled into the cavity. Accordingly, CRDS with coherent cw excitation is most useful when tunable low-power lasers are employed which exhibit a narrow linewidth in the order of the cavity transmission bandwidth. For example, the instantaneous spectral mode width of a 1m-long cavity with $R=99.9\%$ mirrors is 48 kHz. In order to periodically repeat the leak-out events the cavity mode must be frequency-locked to the laser.

A major benefit of this method is the very high spectral resolution inherently provided. The spectral resolution of conventional pulsed CRDS is usually limited by the spectral width of the laser pulse, i.e., several GHz. Only under special conditions one can achieve CRDS spectra with a resolution greater than that of the pulsed laser source.²² In contrast, with coherent cw excitation of a single cavity mode the resolution is only limited by the bandwidth of the cavity resonance mode which may be 10 kHz or less, depending on the mirror reflectivity.

It should be noted that several other experimental arrangements have been recently investigated that make use of cw lasers, some of them employing cavities with a very dense transverse mode structure.²³ In order to clearly distinguish our experimental approach, where the laser is locked to a single fundamental cavity mode, from other techniques we prefer to call this “CAvity Leak-Out Spectroscopy” (CALOS) which we find more appropriate than “cw-CRDS”.

3. EXPERIMENTAL

The experimental setup is schematically shown in Figure 3.1. The main components are the tunable mid-infrared laser system, the ring-down cell, and the photodetector with data acquisition electronics.

3.1. Laser system

This work was carried out with a CO overtone laser with optional electro-optic sideband modulator (EOM) (Zitat). The CO overtone laser is based on a liquid-nitrogen-cooled gain tube (length: 1.5 m) in a cavity formed by a reflection grating (450 lines/mm) in a Littrow mount and a 10m-radius output coupler ($R=98\%$). The grating provides intracavity selection of the laser line, and the output coupler is mounted upon a piezoceramic transducer (PZT) to enable fine frequency control. The laser gas, a mixture of He, N₂, CO, and air, is pumped through the laser tube and excited by a DC discharge. Detailed considerations of the laser operation can be found elsewhere²⁴. More than 350 laser lines are available in the spectral region between 2.6 and 4.1 μm , with single-mode output powers of 40 to 400 mW depending on the vibrational band and the J value of the lasing transition. The spectral linewidth of the CO laser radiation has been measured via a heterodyne experiment.²⁵

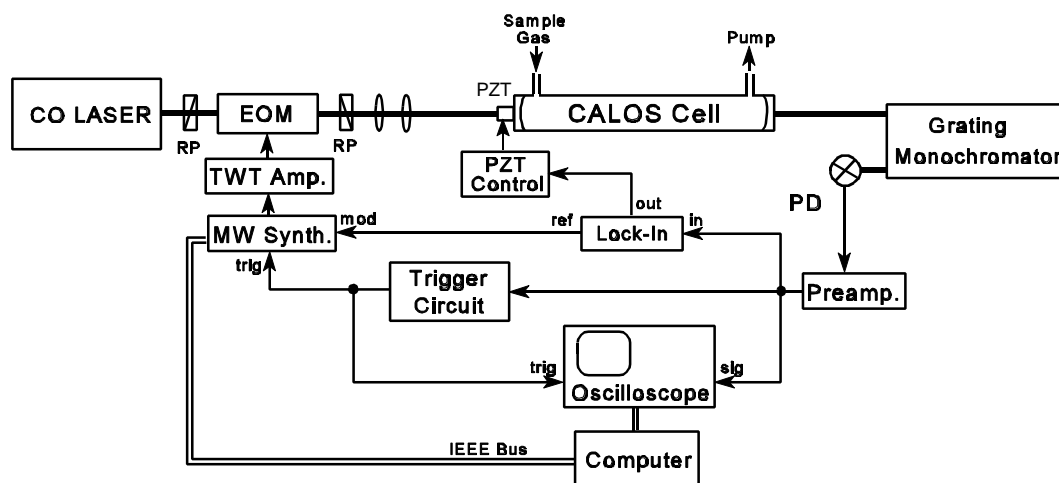


Fig. 3.1: Schematic of the experimental setup, PZT: Piezoceramic transducer, PD: Photodetector, TWT Amp.: Traveling-wave tube amplifier, MW Synth.: Microwave synthesizer, EOM: Electro-optic modulator, RP: Rochon polarizer.

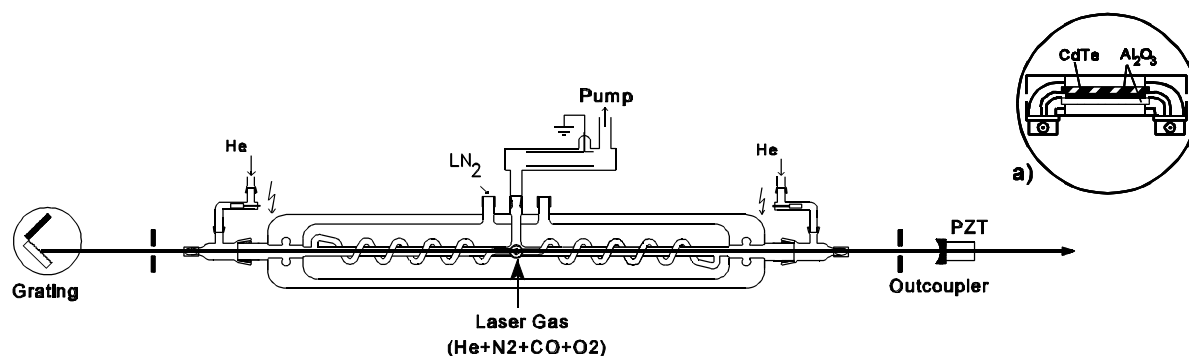


Fig. 3.2: Setup of the CO overtone laser. Inset (a): design of the electro-optic sideband modulator

This measurement indicated a linewidth of about 100 kHz in an observation interval of 1 s.

The electro-optic sideband modulator, depicted in inset (a) of Fig. 3.2, consists of a CdTe crystal (dimensions: 40 mm x 3 mm x 3 mm), mounted in a rectangular microwave waveguide. The design of this traveling-wave modulator follows the example of Magerl and coworkers.²⁶ The CdTe crystal is embedded between two Al₂O₃ slabs which roughly have the same dielectric constant as the mixing crystal. The waveguide is designed to match the velocity of laser light and microwave radiation for microwave frequencies of 8 to 18 GHz. The crystal is cut for amplitude modulation and located between two crossed Rochon prism polarizers. Thus, the modulator generates two sidebands which are continuously tunable between 8 and 18 GHz above and below the laser frequency. The microwave frequency is generated by a commercial 2-20 GHz frequency synthesizer and amplified in a traveling-wave tube amplifier to a power of about 20 W at the EOM crystal. With 200 mW laser power near 3 μm and 20 W of microwave power we obtain about 100 to 200 μW for each sideband depending on the microwave frequency. The EOM also serves as a fast optical switch. Shut-down of the microwave power turns off the sidebands with a response time of about 500 ns. During the stage of this work when we used the solitary CO laser without EOM we used an acousto-optical modulator (AOM) as fast optical switch (response time: ca. 100 ns).

3.2. Ring-down cell

The ring-down cell is completely made of stainless steel, a cross section is depicted in Fig. 3.3. The sample gas is piped through the cell via two bores, the flow rate is determined by an external flow meter. The mirrors used in this work are 0.8"-diameter plano-concave mirrors with 6 m radii of curvature, HR coated at the curved side for $R=99.98\%$ reflectivity at 3.3 μm, and AR coated on the plane side. The usable wavelength region reaches from 3.0 to 3.6 μm. The mirror distance is 0.7 m, corresponding to a free spectral range of 214 MHz. The mirrors are attached to kinematic mounts which are fixed on a cylindrical stainless steel tube. One mirror is mounted on a PZT to enable fine control of the mirror distance. For operation at low pressure the cell can be sealed via two flanges with two stainless steel endpieces which hold AR-coated optical windows. Since the mirrors sit completely inside the cell, the alignment of the mirrors is not affected when the pressure inside the cell is changed. Measurements below ambient pressure is of advantage since pressure broadening is reduced which allows for better separation of neighboring spectral lines belonging to different molecular species.

3.3. Optical setup and data acquisition

The laser light is transversally mode-matched to the fundamental TEM₀₀ modes of the ring-down cavity by means of two appropriate lenses. The light transmitted through the cavity is directed to a LN₂-cooled InSb photodiode. Unfortunately, a fraction of only 1 - 2% of the incident light is transmitted through the cavity on resonance. We speculate that the absorption and scattering processes in the mirrors are responsible for the photon loss. Also, the frequency jitter of the laser line may contribute to this rather low coupling efficiency. Nevertheless, with a power of about 100 μW in one of the laser sidebands

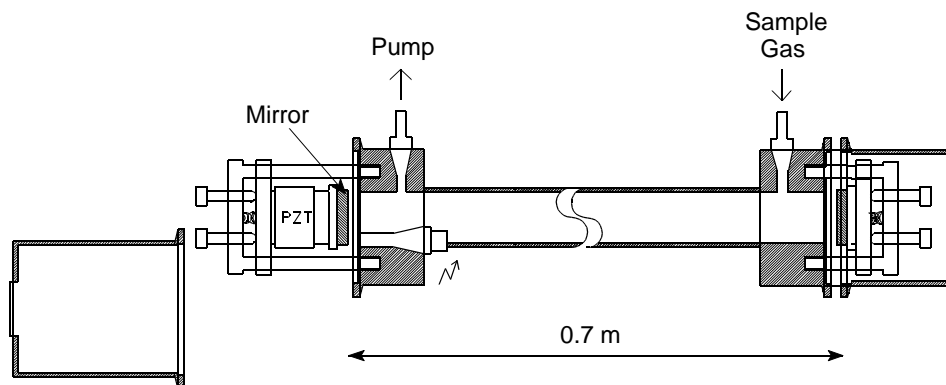


Fig. 3.3: Cross-section of the ring-down cell. The cell is entirely made of stainless steel. One of the mirrors sits on a PZT for fine control of the cavity length. One of the endpieces is demounted.

the signal-to-noise ratio is still sufficient to reliably observe leak-out signals. Since the sideband modulator generates two sidebands (above and below the laser frequency), the sideband of interest is selected with a grating monochromator (0.5m-Czerny-Turner configuration). The monochromator is located between the RDC and the photodetector.

In order to achieve locking of a cavity resonance to the laser frequency, the laser frequency is sinusoidally modulated with 200 Hz. Frequency stabilization of the cavity resonance to the (center) frequency of the laser light is

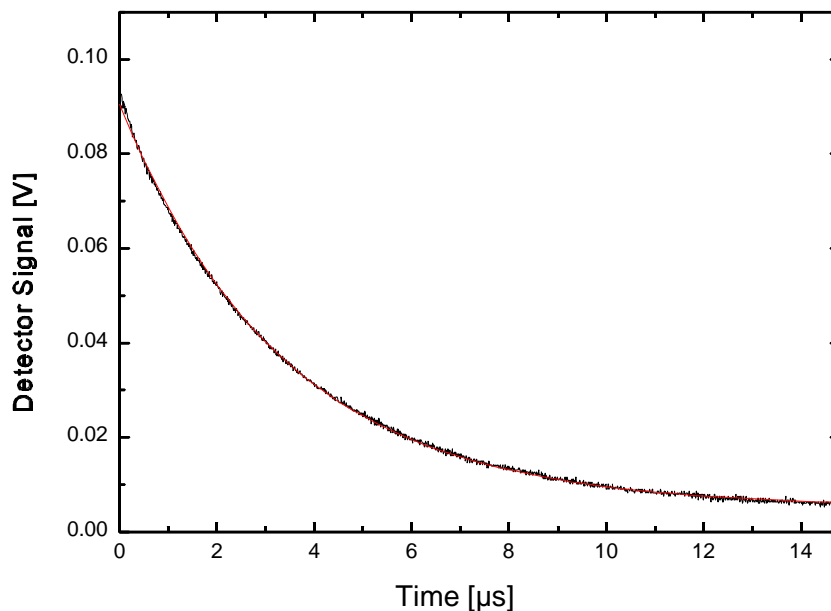


Fig. 3.4: Record of a typical cavity leak-out signal. Signal averages: 100. The experimental data are fitted by an exponential.

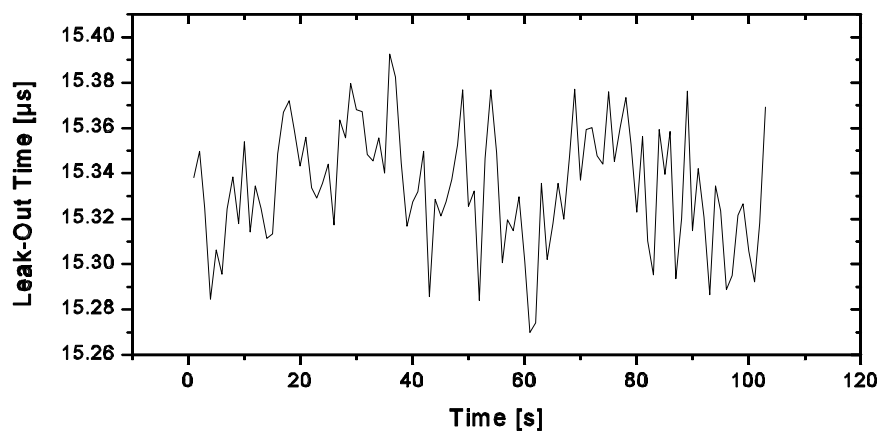


Fig. 3.5: Plot of the empty cavity decay time vs. time. The standard deviation is 1.7×10^{-3} , corresponding to a noise equivalent absorption of $5 \times 10^{-9}/\text{cm}$.

accomplished by means of a standard *If* lock-in technique. Slow thermal drifts of the cavity can thus be corrected. In this way the laser power is periodically injected into the RDC twice per modulation period. Each time the transmitted light indicates optimum coincidence of laser frequency and cavity mode, a trigger pulse is provided to turn off the laser light via the optical switch (EOM or AOM). Simultaneously, this pulse triggers a digital storage oscilloscope with a 2GSa/s sampling rate and an 8-bit vertical resolution for sampling and digitizing the leak-out signal. The signal is typically averaged 100 times, which yields to a data acquisition time of about 2 s. The data are transferred to a PC and analyzed by fitting the signal with a nonlinear Levenberg-Marquardt fit to determine the decay time. These calculations as well as the control of the experiment are carried out by means of the graphical programming language LabVIEW. A typical record of a leak-out signal is depicted in Fig. 3.4. The curve shape is a single exponential decay. The decay time is $3.2 \mu\text{s}$ in this case. If the RDC is evacuated the observed decay time is around $12 \mu\text{s}$, corresponding to a mirror reflectivity of $R=99.98\%$.

A continuous measurement of the leak-out decay rate exhibits fluctuations mainly caused by slight random distortions of the optical cavity geometry due to acoustical jitter (Fig. 3.5). The 1σ -standard deviation during an observation time of 250 s amounts to 1.7×10^{-3} . This baseline jitter corresponds to a noise equivalent absorption of $5 \times 10^{-9}/\text{cm}$.

3.4. Trace gas detection

Since our main interest is focused on the detection of volatile organic compounds (VOC's) in ambient air we studied the performance of the CALOS setup with diluted samples of small hydrocarbons, like methane, ethylene, etc. To characterize the spectrometer we recorded fingerprint spectra from several certified sample gas mixtures at ambient pressure. During one measurement cycle the cavity was successively flushed with pure nitrogen, the sample gas mixture, and pure nitrogen again. This procedure provides a check for systematic changes (drifts) of the empty cavity decay rate. Fig. 3.6. shows an example of such a measurement cycle with a sample gas mixture of 500 ppb ethylene in nitrogen (grade 5). The laser was operating on the P(13) transition of the 26-24 vibrational band, corresponding to a laser frequency $2988,467 \text{ cm}^{-1}$. The sideband modulator was not used at this stage of the experiment. The flow rate was 30 l/h. Correspondingly the time to completely exchange the cell volume is 90 s. Due to absorption the ring-down time falls from τ_0 during nitrogen flow to τ_1 during sample gas flow. The absorption coefficient is determined from the change of the decay rate according to

$$\alpha = 1/c (1/\tau_1 - 1/\tau_0).$$

For this example the measurement yielded $\alpha=3.29(2) \times 10^{-6}/\text{cm}$. According to the HITRAN96 database²⁷ this corresponds to a concentration of 553(4) ppb which is in good agreement with the certified concentration of 523 ppb \pm 10%. To obtain a

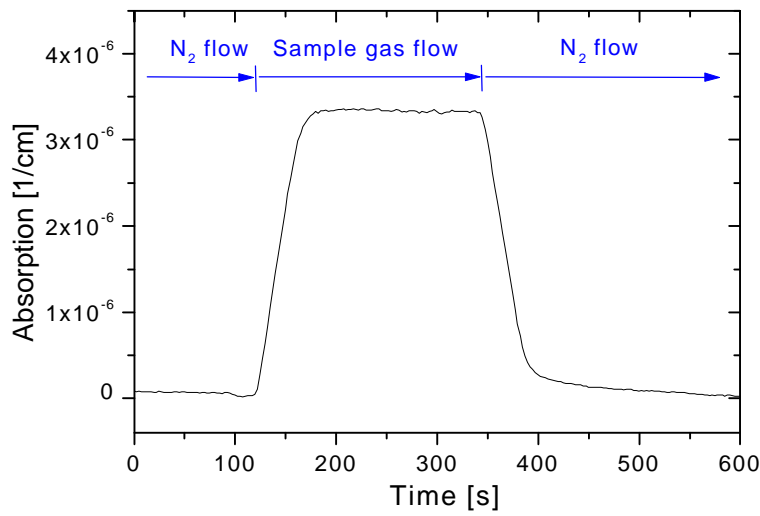


Fig. 3.6: Absorption measurement of sample gas mixture at atmospheric pressure. Sample gas mixture: 500 ppb ethylene in nitrogen, CO overtone laser line: P(13), 26-24 band.

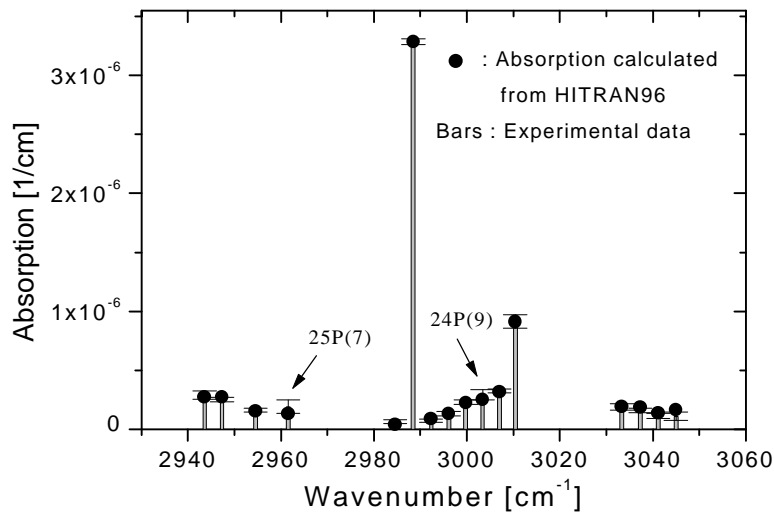


Fig. 3.7: Cavity leak-out fingerprint spectrum of ethylene in the spectral region around 3000 cm^{-1} at atmospheric pressure. Ethylene concentration was 553 ppb in nitrogen. The error bars indicate the 1σ -uncertainty of the measurements. For comparison, the absorption calculated from HITRAN96 are plotted as dots.

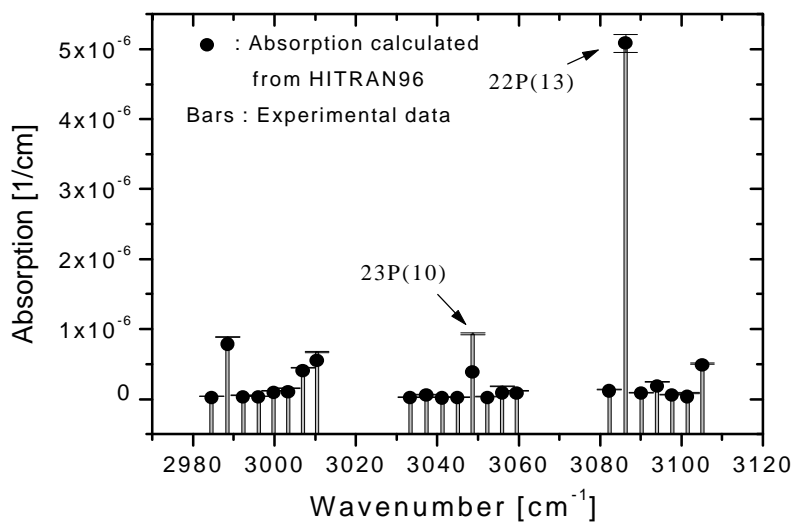


Fig. 3.8: Cavity leak-out fingerprint spectrum of methane in the spectral region around 3000 cm^{-1} at atmospheric pressure. Methane concentration was 974 ppb in nitrogen. The error bars indicate the 1σ -uncertainty of the measurements. For comparison, the absorption calculated from HITRAN96 are plotted as dots.

fingerprint spectrum, the procedure described above was repeated for several CO overtone laser lines between 2940 and 3050 cm^{-1} . In Fig. 3.7 the measured absorption coefficient is plotted vs. frequency of the laser lines. The α values calculated from the HITRAN96 database are also plotted for comparison. The agreement is almost perfect, with exception of the lines 25P(7) and 24P(9) where the absorption measured is significantly higher than calculated from HITRAN. We attribute this to additional absorption due to residual water in the sample gas mixture. The noise-equivalent absorption varied between $5 \times 10^{-9}/\text{cm}$ and $1 \times 10^{-8}/\text{cm}$ (integration time: 100 s) which corresponds to a minimum detectable ethylene concentration of about 1 ppb. The same type of measurement has been performed with a sample gas mixture of 1 ppm methane in nitrogen. Here we also found very good agreement with the HITRAN96 data (Fig. 3.7). The detection limit for methane is also in the order of 1 ppb. The good agreement with the HITRAN data indicate that the spectrometer responses linearly over the given range of absorption losses and that sensitive and quantitative measurements are feasible.

5. CONCLUSION AND PROSPECTS

In this paper we presented our recent progress towards cavity ring-down spectroscopy with a cw laser near 3 μm . With this approach we realize an optical pathlength of about 4 km in a 70cm-long cell. The high transmission of the RDC on resonance enables the use of tunable low-power laser radiation (cw power < 100 μW) for very sensitive absorption measurements. We demonstrated online-monitoring of trace amounts of various hydrocarbons, e.g., methane, ethylene, at the ppb level. The absorption spectra observed are quantitatively in very good agreement with data calculated from HITRAN96. Up to now the experiments have been performed with a CO overtone laser with optional sideband generation. To achieve portability of the instrument a difference frequency laser system is currently under construction in our laboratory. This laser system is based on difference frequency generation between a Nd:YAG-Laser and a tunable extended-cavity diode laser in a periodically-poled lithium-niobate (PPLN) crystal. The combination of such a compact cw laser system with the CALOS method seems very promising for real-time *in situ* monitoring of trace gases. However, when monitoring atmospheric trace gases in ambient air one has to cope with the additional problem of cross sensitivity. In some cases the spectral lines of different molecules overlap even at reduced pressure which prevents a selective detection and leads to measurements errors. This may be avoided in some cases by going to a slightly different wavelength where the lines are well separated, depending on the molecules of interest and the fractions of other molecules in the sample. Obviously, to perform absorption measurements at the optimum wavelength, the use of a *tunable* laser is essential. The investigation of these problems with CALOS trace gas monitoring in atmospheric air is currently in progress in our laboratory.

ACKNOWLEDGMENT

This work is supported by the German Federal Foundation for Environmental Research (Deutsche Bundestiftung Umwelt). Cooperation of Dr. Bertold Frech and Hannes Dahnke during part of this work is appreciated.

REFERENCES

1. A. O'Keefe, D.A.G. Deacon, "Cavity ring-down optical spectrometer for absorption measurements using pulsed laser sources", *Rev. Sci. Instrum.* **59**, pp. 2544, (1988).
2. P. Zalicki, R.N. Zare, "Cavity ring-down spectroscopy for quantitative absorption measurements", *J. Chem. Phys.* **102**, pp. 2708, (1995).
3. R.T. Jongma, M.G.H. Boogaarts, I. Holleman, G. Meijer, "Trace gas detection with cavity ring-down spectroscopy", *Rev. Sci. Instrum.* **66**, pp. 2821, (1995).
4. J.J. Scherer, J.B. Paul, A. O'Keefe, R.J. Saykally, "Cavity ringdown laser absorption spectroscopy: history, development, and application to pulsed molecular beams", *Chem. Rev.* **97**, pp. 25, (1997).
5. D. Romanini, K. Lehmann, "Ring-down cavity absorption spectroscopy of the very weak HCN overtone bands with six, seven, and eight stretching quanta", *J. Chem. Phys.* **99**, pp. 6287, (1993).
6. G. Meijer, M.G.H. Boogaarts, R.T. Jongma, D.H. Parker, "Coherent cavity ring down spectroscopy", *Chem. Phys. Lett.* **217**, pp. 112, (1994).
7. D. Romanini, K. Lehmann, "Cavity ring-down overtone spectroscopy of HCN, H^{13}CN and HC^{15}N ", *J. Chem. Phys.* **102**, pp. 633, (1995).

8. L. Lehr, P. Hering, "Cavity ring-down spectroscopy of photochemically produced NaH for the determination of relative dipole transition moments", *Appl. Phys. B.* **65**, pp. 595, (1997).
9. N. Seiser, D.C. Robie, "Pressure broadening in the oxygen $b^1\Sigma(v=1) \leftarrow X^3\Sigma(v=0)$ band measured by cavity ring-down spectroscopy", *Chem. Phys. Lett.* **282**, pp. 263, (1998).
10. M.D. Wheeler, S.M. Newman, T. Ishiwata, M. Kawasaki, A.J. Orr-Ewing, "Cavity ring-down spectroscopy of the $A^2\Pi_{3/2} - X^2\Pi_{3/2}$ transition of BrO", *Chem. Phys. Lett.* **285**, pp. 346, (1998).
11. E.R. Crosson, P. Haar, G.A. Marcus, H.A. Schwettman, B.A. Paldus, T.G. Spence, R.N. Zare, "Pulse-stacked cavity ring-down spectroscopy", *Rev. Sci. Instrum.* **70**, pp. 4, (1999).
12. J.J. Scherer, D. Voelkel, D.J. Rakestraw, J.B. Paul, C.P. Collier, R.J. Saykally, A. O'Keefe, "Infrared cavity ring down laser absorption spectroscopy (IR-CRLAS)", *Chem. Phys. Lett.* **245**, pp. 273, (1995).
13. J.J. Scherer, D. Voelkel, D.J. Rakestraw, "Infrared cavity ringdown laser absorption spectroscopy (IR-CRLAS) in low pressure flames", *Appl. Phys. B.* **64**, pp. 699, (1997).
14. K. Lehmann, U.S. Patent 5528040, (1996).
15. R. Engeln, G. von Helden, G. Berden, G. Meijer, "Phase shift cavity ring down absorption spectroscopy", *Chem. Phys. Lett.* **262**, pp. 105, (1996).
16. B.A. Paldus, J.S. Harris, J. Martin, J. Xie, R.N. Zare, "Laser diode cavity ring-down spectroscopy using acousto-optic modulator stabilization", *J. Appl. Phys.* **82**, pp. 3199, (1997).
17. D. Romanini, A.A. Kachanov, N. Sadeghi, F. Stoeckel, "Cw cavity ring down spectroscopy", *Chem. Phys. Lett.* **264**, pp. 316, (1997).
18. D. Romanini, A.A. Kachanov, F. Stoeckel, "Diode laser cavity ring down spectroscopy", *Chem. Phys. Lett.* **270**, pp. 538, (1997).
19. Y. He, M. Hippler, M. Quack, "High-resolution cavity ring-down absorption spectroscopy of nitrous oxide and chloroform using a near-infrared cw diode laser", *Chem. Phys. Lett.* **289**, pp. 527, (1998).
20. B.A. Paldus, C.C. Harb, T.G. Spence, B. Wilke, J. Xie, J.S. Harris, R.N. Zare, "Cavity-locked ring-down spectroscopy", *J. Appl. Phys.* **83**, pp. 3991, (1998).
21. M. Mürtz, B. Frech, W. Urban, "High-resolution cavity leak-out absorption spectroscopy in the 10 μm region", *Appl. Phys. B.* **68**, pp. 243, (1999).
22. K. Lehmann, D. Romanini, "The superposition principle and cavity ring-down spectroscopy", *J. Chem. Phys.* **105**, pp. 10263, (1996).
23. R. Engeln, G. Berden, R. Peeters, G. Meijer, "Cavity enhanced absorption and cavity enhanced magnetic rotation spectroscopy", *Rev. Sci. Instrum.* **69**, pp. 3763, (1998).
24. W. Urban, "The CO overtone laser: a spectroscopic source in a most interesting wavelength region", *Applied laser spectroscopy*, W. Demtröder, M. Inguscio, pp. 127, Plenum, New York, (1990).
25. M. Mürtz, B. Frech, P. Palm, R. Lotze, W. Urban, "Tunable carbon monoxide overtone laser sideband system for precision spectroscopy from 2.6 to 4.1 μm ", *Opt. Lett.* **23**, pp. 58, (1998).
26. G. Magerl, W. Schupita, E. Bonek, "A tunable CO₂ laser sideband spectrometer", *IEEE J. Quantum Electron.* **18**, pp. 1214, (1982).
27. <http://www.hitran.com>.